



Identification of MK-5710 ((8*aS*)-8*a*-methyl-1,3-dioxo-2-[(1*S*,2*R*)-2-phenylcyclopropyl]-*N*-(1-phenyl-1*H*-pyrazol-5-yl)hexahydro-imidazo[1,5-*a*]pyrazine-7(1*H*)-carboxamide), a potent smoothed antagonist for use in Hedgehog pathway dependent malignancies, Part 2

Olaf Kinzel, Anna Alfieri, Sergio Altamura, Mirko Brunetti, Simone Bufali, Fabrizio Colaceci, Federica Ferrigno, Gessica Filocamo, Massimiliano Fonsi, Paola Gallinari, Savina Malancona, Jose Ignacio Martin Hernando, Edith Monteagudo, Maria Vittoria Orsale, Maria Cecilia Palumbi, Vincenzo Pucci, Michael Rowley, Romina Sasso, Rita Scarpelli, Christian Steinkühler, Philip Jones*

IRBM, Merck Research Laboratories Rome, Via Pontina km 30,600, Pomezia, 00040 Rome, Italy

ARTICLE INFO

Article history:

Available online 16 June 2011

Keywords:

Hedgehog pathway
Smoothed antagonist
Hedgehog inhibitor

ABSTRACT

The Hedgehog (Hh-) signaling pathway is a key developmental pathway which gets reactivated in many human tumors, and smoothed (Smo) antagonists are emerging as novel agents for the treatment of malignancies dependent on the Hh-pathway, with the most advanced compounds demonstrating encouraging results in initial clinical trials. A novel series of potent bicyclic hydantoin Smo antagonists was reported in the preceding article, these have been resolved, and optimized to identify potent homochiral derivatives with clean off-target profiles and good pharmacokinetic properties in preclinical species. While showing in vivo efficacy in mouse allograft models, unsubstituted bicyclic tetrahydroimidazo[1,5-*a*]pyrazine-1,3(2*H*,5*H*)-diones were shown to epimerize in plasma. Alkylation of the C-8 position blocks this epimerization, resulting in the identification of MK-5710 (**47**) which was selected for further development.

© 2011 Elsevier Ltd. All rights reserved.

The hedgehog (Hh-) signaling pathway is a one of several key developmental pathways which regulate patterning, growth and cell migration in most tissues and organs, and while it plays an important role during embryonic development its role in adulthood is limited to a tissue maintenance and repair.^{1–4} Hh-signal transduction is initiated by binding of the Hh-protein to its cellular membrane receptor Patched (Ptch), thereafter binding relieves Ptch-mediated repression of the GPCR-like receptor smoothed (Smo). Activation of Smo then initiates an intracellular signalling cascade, culminating in the translocation of the Gli-transcription factors, Gli-1, -2, into the nucleus where they regulate genes involved in differentiation, proliferation and survival. Evidence has emerged showing that the pathway is aberrantly activated in a wide number of cancers, through mutations in Ptch and Smo, as well as downstream factors SUFU and Gli.^{1,2} Several agents have been demonstrated to show preclinical antitumor activity in animal models,^{3,5} including the natural product cyclopamine, and var-

ious synthetic Smo antagonists. Recently, the most advanced of these, vismodegib (GDC-0449),⁶ has demonstrated encouraging results in phase I studies in advanced basal cell carcinoma.⁷ These results suggest blockage of the Hh-pathway is an attractive approach to target defined tumors dependent on this pathway.

We have previously reported the identification and initial SAR exploration of a novel series of [6,5]-bicyclic tetrahydroimidazo[1,5-*a*]pyrazine-1,3(2*H*,5*H*)-dione smoothed antagonists with potential for the treatment of Hh-pathway dependent malignancies, exemplified by **1** and **2** (Fig.1).⁸

This article describes the subsequent optimization of this series of hydantoins Smo antagonists, culminating in identification of the

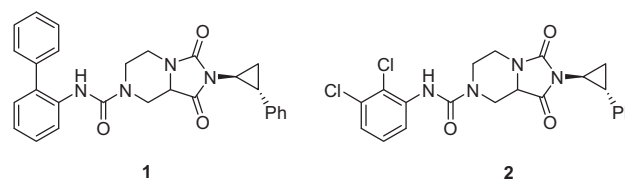


Figure 1. Lead Smo antagonists.

* Corresponding author at present address: Belfer Institute for Applied Cancer Sciences, Dana Farber Cancer Institute, 450 Brookline Avenue, Boston, MA 02115, USA. Tel.: +1 617 582 9648.

E-mail address: philip_jones@dfci.harvard.edu (P. Jones).

Table 1
Biological activities of lead Smo antagonists, and their individual stereoisomers^a

Compd	Light2 IC ₅₀ (nM)	Smo Bind 2% FCS IC ₅₀ (nM)
1	84	94
2	340	220
3 (Single isomer of 1)	100	48
4 (8 <i>aS</i> , 1 <i>S</i> , 2 <i>R</i> isomer of 1)	42	21
5 (Single isomer of 1)	140	95
6 (Single isomer of 1)	50	35
7	270	230
8	880	670
9	430	650
10	1400	1700

^a Values are means of at least five experiments (SD were within 25% of the IC₅₀ values).

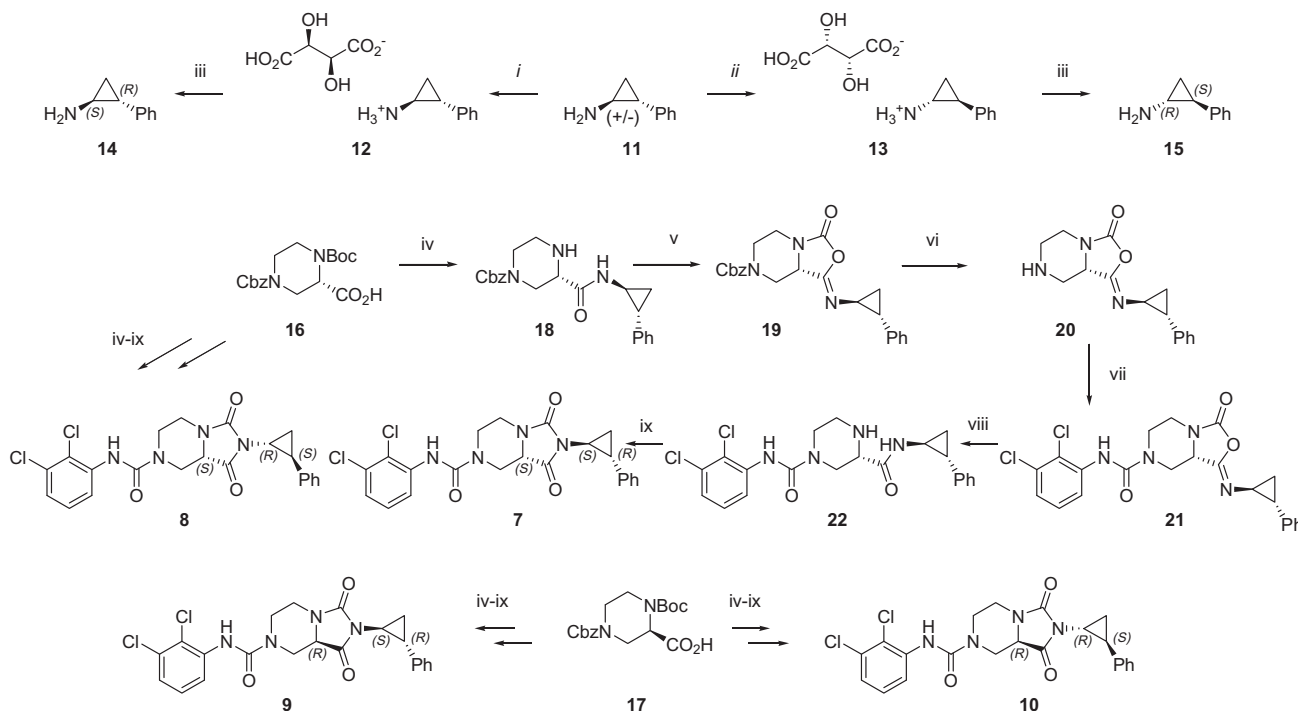
preclinical candidate MK-5710 (**47**) that displays good pharmacokinetics in preclinical species, demonstrates sustained target engagement *in vivo*, and striking anti-tumor efficacy in a mouse allograft tumor model dependent on the Hh-signalling pathway.

One of the initial tasks of the lead optimization program was to determine which of the stereoisomers of **1** and **2** was responsible for the biological activity, as the initial characterization of these compounds was conducted on mixtures of four stereoisomers resulting from the hydantoin chiral centre and racemic *trans* 2-phenylcyclopropylamine. Consequently, the mixture of biphenyl urea **1** was deconvoluted to the stereoisomers **3–6** by chiral supercritical fluid chromatography (SFC).⁹ The individual stereoisomers were profiled in both a reporter gene assay in an engineered mouse NIH 3T3 cell line stably incorporating a Gli-dependent firefly luciferase reporter gene where the ability of the compounds to inhibit Hh-signalling following activation with the agonist Purmorphamine is measured (Light2),¹⁰ and in a Smo binding assay where the ability of the antagonists to displace a fluorescently labeled

bodipy-cyclopamine from HEK-293 cells expressing recombinant human Smo is measured (Smo Bind).¹¹ The latter was conducted in 2% fetal calf serum (FCS), and also in 20% normal human serum (NHS). The individual stereoisomers displayed slight differences in activity, around a 4-fold difference (Table 1).

In parallel, a chiral synthesis of the four individual stereoisomers was conducted to yield **7–10** (Scheme 1). Firstly, *trans* 2-phenylcyclopropylamine **11** was resolved into its individual tartaric acid salts **12** and **13** as described by Newman,¹² and converted to the corresponding free amines (**14** and **15**). In turn, each enantiomer was coupled with homochiral 4-[(benzyloxy)carbonyl]-1-(*tert*-butoxycarbonyl)piperazine-2-carboxylic acids **16** and **17**. Following removal of the Boc-protecting group, cyclization to the desired hydantoin using triphosgene at rt was attempted. Instead of closure to the desired bicyclic scaffold, cyclization occurred on the amide oxygen atom to give the isomeric 1-imino-3-oxotetrahydro[1,3]oxazolo[3,4-*a*]pyrazine core **19** in modest yield. This material was carried forward, and following removal of the protecting group and urea formation, the five membered ring was reopened to homochiral piperazine carboxamide **22** by stirring with 0.2 M HCl in dioxane for 1 h at rt. Ring closure with two equivalents of triphosgene in the presence of DBU in DCM at –30 to –10 °C successfully yielded the required bicyclic hydantoin **7** after 45 min, with high stereochemical purity (>90% de by chiral SFC). Similar results were obtained during the preparation of stereoisomers **8–10**.

The four stereoisomers displayed a similar four fold shift in activity from the most potent to the weakest Smo antagonist (Table 1). The stereochemistry of the 2-phenylcyclopropylamine proved to be the key determinant for activity as the pair of compounds bearing the 1*S*,2*R* stereochemistry (**7** and **9**) displayed the highest affinity. The chiral centre on the bicyclic framework influenced the activity to a limited extent, with the *S*-stereochemistry (**7**) being the more active configuration. The *R*-diastereomer (**9**) was around two fold weaker than **7** in both Light2 (IC₅₀ = 270



Scheme 1. Initial synthetic procedure towards single stereoisomeric Smo antagonists. Reagents and conditions: (i) D-tartaric acid, EtOH, Δ, then three recrystallizations, EtOH/H₂O (4:1) (31%). (ii) L-tartaric acid, EtOH, Δ, then three recrystallizations, EtOH/H₂O (4:1) (32%). (iii) 2 N NaOH/Et₂O (95%). (iv) HATU, DIPEA, DMF; then TFA/DCM (85–99%). (v) 0.33 equiv triphosgene, 10 equiv DIPEA, DCM, rt (48–55%) (vi) H₂, Pd/C, MeOH (quant.). (vii) Ar-NCO, DIPEA, DCE (50–76%). (viii) 0.2 M HCl, dioxane (quant.). (ix) 2 equiv triphosgene, 5 equiv DBU, DCM, –30 to –10 °C (10–55%).

and 430 nM) and Smo binding assays (230 and 640 nM respectively). Subsequent synthesis revealed that the most active biphenyl urea **4** also displayed the 8*a*S, 1*S*, 2*R* stereochemistry (Scheme 2). Subsequently, further SAR was conducted using this stereoisomer (Table 2).

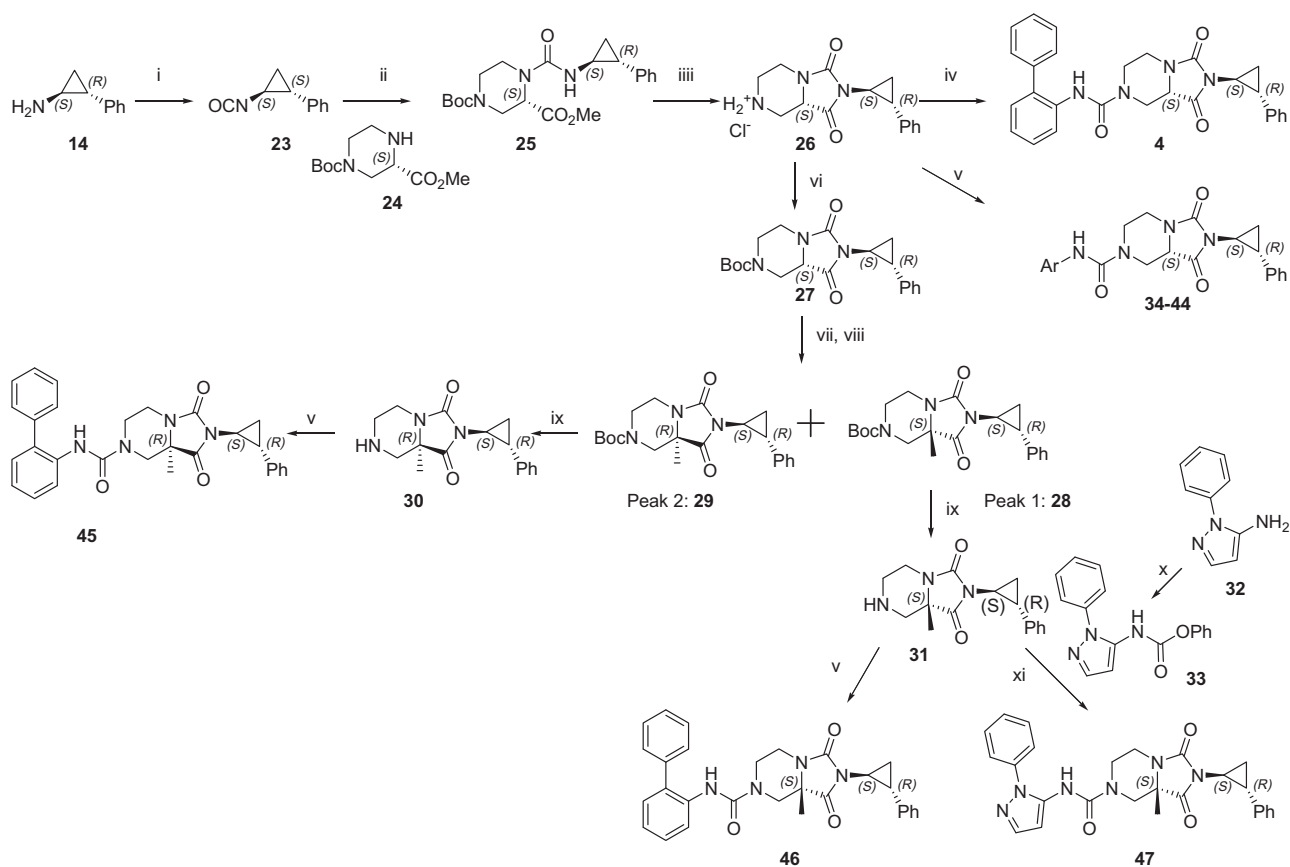
A more robust synthetic pathway to the desired homochiral framework was established (Scheme 2), whereby the homochiral 1*S*,2*R* 2-phenylcyclopropylamine **14** was converted to the corresponding isocyanate **23** with triphosgene. Reaction with 1-*tert*-butyl 3-methyl (3*S*)-piperazine-1,3-dicarboxylate **24** gave first the corresponding urea **25**, which could then be cyclized with 4 M HCl in dioxane to give the hydantoin scaffold **26** in excellent yield and high stereochemical purity. Coupling with the desired isocyanate formed the required Smo antagonists in good yield, for example reaction with [1,1'-biphenyl]-2-yl-isocyanate gave **4** in 67% yield, 92% de.

Given the interest in **4** and **7** they were extensively profiled. Both compounds were able to inhibit the proliferation of irradiated Ptch +/- medulloblastoma cells with CC₅₀ = 2 and 12 nM respectively.¹³ The biphenyl derivatives typically proved to be the more potent analogues, and **4** displayed IC₅₀ = 21 nM in the binding assay in the presence of 2% FBS, with around a 3-fold serum shift in the presence of 20% NHS, IC₅₀ = 70 nM, reflecting the relatively high plasma protein binding (PPB), *f*_u = 4.4%. This derivative displayed low microsomal stability, with Cl_{int} >300 and 120 μL/min/mgP in rat and human microsomes respectively, and relatively high clearance in rats, Cl = 56 mL/min/kg (Table 3). Furthermore, **4** was also a weak inhibitor of CYP450s 2C9 and 3A4, 50% inhibition at 10 μM.

On the other hand, the 2,3-dichloroanilide **7** although displayed slightly inferior affinity, with Smo binding IC₅₀ = 230/690 nM (2% FBS/20% NHS), it proved to have more benign pharmacokinetics profile. In liver microsomes, **7** displayed modest turnovers with Cl_{int} = 170, 105, and 73 μL/min/mgP in rat, dog and human microsomes respectively. In vivo in both rats and dogs low-moderate clearances were measured, 46 and 4 mL/min/kg respectively. The compound displayed acceptable bioavailability (*F* = 30%) and *T*_{1/2} = 2.2 h in rats; and excellent bioavailability (*F* = 97%) and long terminal half life in dogs, *T*_{1/2} = 10 h. In ancillary screening both compounds displayed micromolar activity on I_{Kr}, I_{Ks} and Cav1.2 cardiac ion channels, as well binding to the adenosine transporter and histamine H1.

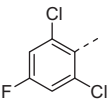
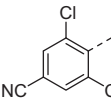
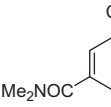
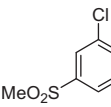
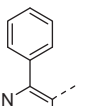
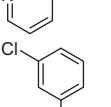
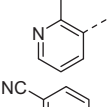
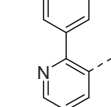
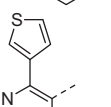
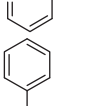
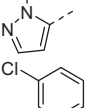
In the interests of optimizing this series further (Table 2), SAR was conducted with the aims to improve the pharmacokinetics properties in the bi(hetero)aryl ureas, and improving the potency whilst maintaining the good PK profile in the monoaryl ureas. In both cases given the relatively high lipophilicity of these compounds with high PPB and micromolar ion channel activity and CYP inhibition, efforts focused on the introduction of polar groups and heteroatoms, building on previous knowledge from the racemic series.⁸

In the monoaryl series derivatives **34–37** were prepared introducing the electron deficient substituents in the *para* position of a 2,6-dichloroanilide. All four derivatives displayed higher affinity than **7**, most notably the dimethylcarboxamide **36**, and the methylsulfone **37**, both of which displayed double digit affinity in the Smo binding assay (IC₅₀ = 77 and 42 nM respectively), with the latter displaying minimal serum shift. The introduction of these



Scheme 2. Modified synthetic procedure for the preparation of single stereoisomeric Smo antagonists. Reagents and conditions: (i) triphosgene, NaHCO₃ (aq)/DCM (98%). (ii) DCM, 1 h. (iii) 4 M HCl/dioxane, 2 h (95%, 92%de). (iv) [1,1'-biphenyl]-2-yl-isocyanate, DIPEA, DCM, 1 h (67%, 92%de). (v) [1,1'-biphenyl]-2-yl-isocyanate, DIPEA, DCM, 1 h. (vi) Boc₂O, DIPEA, DCM (quant.). (vii) LiHMDS, THF, -78 °C, 30 min then MeI -78 °C to rt (77%) (viii) Chiral SFC purification. (ix) TFA, DCM. (x) PhOCOCl, DIPEA, DCE, 1 h (94%). (xi) **33**, DCM, Et₃N (90%).

Table 2
Biological activities of homochiral Smo antagonists^a

Compd	Light2 IC ₅₀ (nM) ^a	Smo Bind 2% FCS IC ₅₀ (nM) ^a	Smo Bind 20% NHS IC ₅₀ (nM) ^a	
4	42	21	70	
7	270	230	690	
34		140	180	520
35		120	100	450
36		120	77	120
37		41	42	68
38		28	12	12
39		5	4	15
40		5	16	22
41		89	21	42
42		18	15	18
43		8	18	32
44		6	7	9
45		1400	1200	1600
46		23	19	60
47		17	13	22

^a Values are means of at least five experiments (SD were within 25% of the IC₅₀ values).

trisubstituted anilines also improved the PK properties (Table 3), and all four compounds showed improved stability compared to **7** in liver microsomes, notably **35–37** also displayed lower clearance in rats. Indeed **35** showed remarkable low rat clearance,

Cl = 2 mL/min/kg, but this was probably a result of very high PPB in rats ($f_u = 0.7\%$). The overall profile of **37** in rats was encouraging, with low clearance (Cl = 5 mL/min/kg), excellent oral bioavailability ($F = 74\%$) and moderate half life ($T_{1/2} = 3.2$ h). However, in dogs

Table 3
Pharmacokinetic properties of individual stereoisomeric Smo antagonists

Compd	Microsomes Cl_{int} ($\mu\text{L}/\text{min}/\text{mgP}$)			Rat PK				Dog PK			
	Rat	Dog	Human	Cl ($\text{mL}/\text{min}/\text{kg}$)	$T_{1/2}$ (h)	V_{dss} (L/kg)	F (%)	Cl ($\text{mL}/\text{min}/\text{kg}$)	$T_{1/2}$ (h)	V_{dss} (L/kg)	F (%)
4	>300	ND	120	56	2.7	8	ND				
7	170	105	73	46	2.2	8	30	4	10	2.5	97
34	117	ND	64								
35	109	83	66	2	5.4	0.5	56				
36	58	ND	49	41	0.6	2.1	ND				
37	53	39	58	5	3.2	0.6	74	1.7	1.0	0.3	ND
38	81	60	45	54	4.9	6.7	31				
39	133	147	90	54	1.3	4.1	ND				
40	43	40	37	48	3.8	6	43				
41	91	50	40	58	10	10	41	7.6	3.1	1.0	ND
42	49	39	31	43	1.3	2.9	88	5.5	2.5	1.0	82
43	113	ND	62								
44	80	39	45								
47	55	94	36	22	5.1	2.9	40	22	1.1	2.0	52

despite the low clearance ($Cl = 1.7 \text{ mL}/\text{min}/\text{kg}$) the low volume of distribution resulted in a short terminal half life ($T_{1/2} = 1.0 \text{ h}$).

Previous work had illustrated that 2-aryl-3-aminopyridines and *N*-aryl-5-aminopyrazoles to be suitable replacements to the biphenyl-2-amine,⁸ and accordingly these groups were explored further. As expected, the 2-aryl-3-aminopyridines **38–41** proved to be potent Smo antagonists, with **39** and **40** bearing the *meta* substituents on the remote phenyl ring being some of the most potent

compounds identified, displaying $IC_{50} = 4$ and 16 nM in 2% FCS respectively, and $IC_{50} = 15$ and 22 nM in the high serum conditions. The introduction of the pyridyl group served both to alleviate the micromolar ion channel and CYP inhibition activities, and also to remedy the high microsomal turnover. In rats all four derivatives (**38–41**) displayed clearances in the range 48–58 $\text{mL}/\text{min}/\text{kg}$, but as a result of larger V_{dss} they displayed longer half lives than the corresponding dichloroanilines. Oral bioavailabilities were also

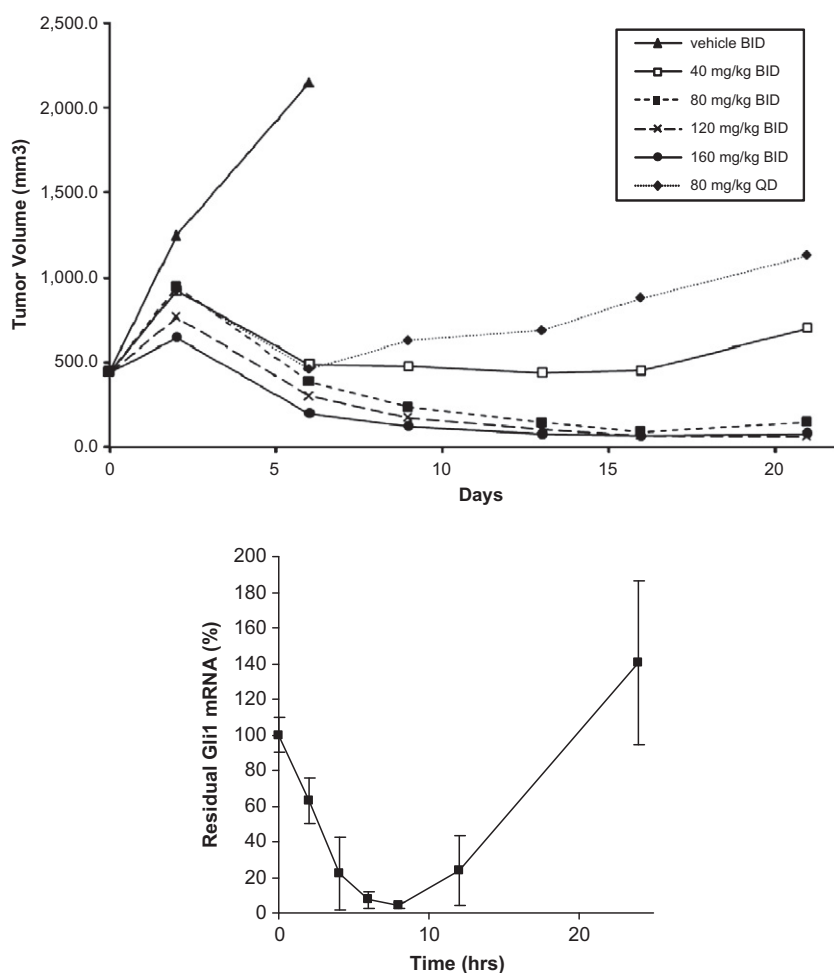


Figure 2. Efficacy of **42** in medulloblastoma bearing mice,¹³ following oral dosing at 40, 80, 120 and 160 mg/kg bid and 80 mg/kg qd as suspension in 0.24% SDS/0.5% Methocel. PD of **42** in tumor biopsies from medulloblastoma bearing mice, following a single oral 80 mg/kg dose.

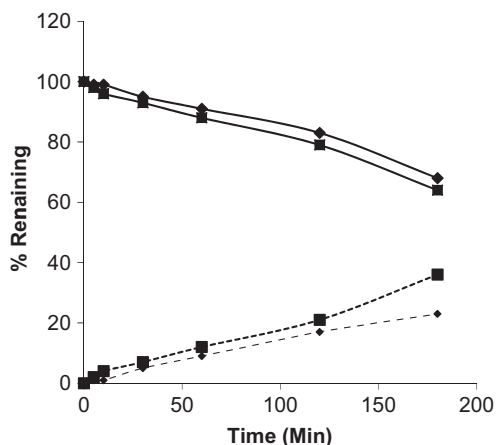


Figure 3. Epimerization of **42** in rat (squares) and human (diamonds) plasma, and formation of diastereomer (dashed lines).

acceptable ($F = 31\text{--}43\%$). Encouraged by the rat PK where **41** displayed a long terminal half life ($T_{1/2} = 10.4$ h), **41** was profiled also in dogs where despite displaying moderate clearance ($Cl = 7.6$ mL/min/kg), the $T_{1/2}$ was a more modest 3.1 h.

Turning attention to the *N*-aryl-5-aminopyrazoles, incorporation of this functionality into the bicyclic hydantoin series gave a

number of very interesting compounds (**42–44**). The prototype **42** proved to be a very potent Smo antagonist, Light2 $IC_{50} = 18$ nM, with no serum shift in the binding assay ($IC_{50} = 15/18$ nM, 2% FCS/20% NHS) as a result of the large free fraction in human plasma, $f_u = 17\%$. Unlike the pyridine series, the introduction of *meta* substituents on the remote phenyl ring had minimal influence on the affinity. All three derivatives were devoid of ion channel and CYP liabilities at 10 μ M, while in microsomal turnover studies all three compounds showed substantial improvements compared to the biphenyl derivative **4**. Interestingly, the *meta* substituted analogues **43** and **44** showed slightly inferior stability compared to the parent **42**. Accordingly **42** was profiled in vivo in both rats and dogs, where it displayed excellent oral bioavailability in both species ($F = 88$ and 82% respectively) with moderate clearance ($Cl = 43$ and 5.5 mL/min/kg) and comparable half lives in both species ($T_{1/2} = 1.3$ and 2.5 h).

In view of the encouraging overall profile **42** was profiled to see if it could inhibit the proliferation of irradiated Ptch \pm medulloblastoma cells which are dependent on the pathway,¹³ and **42** displayed $CC_{50} = 1$ nM. Good exposure of **42** could be obtained in mice upon oral administration ($AUC = 6.4_{[40\text{ mg/kg}]}$, $15_{[80\text{ mg/kg}]}$, $24_{[160\text{ mg/kg}]}$ μ M h), and therefore **42** was evaluated in a primary mouse medulloblastoma allograft model. When the subcutaneous tumors reached an average volume of 400 mm³ mice were randomized and treated orally at 40, 80, 120 and 160 mg/kg bid for 3 weeks, and also 80 mg/kg qd. All doses were well tolerated, with less than

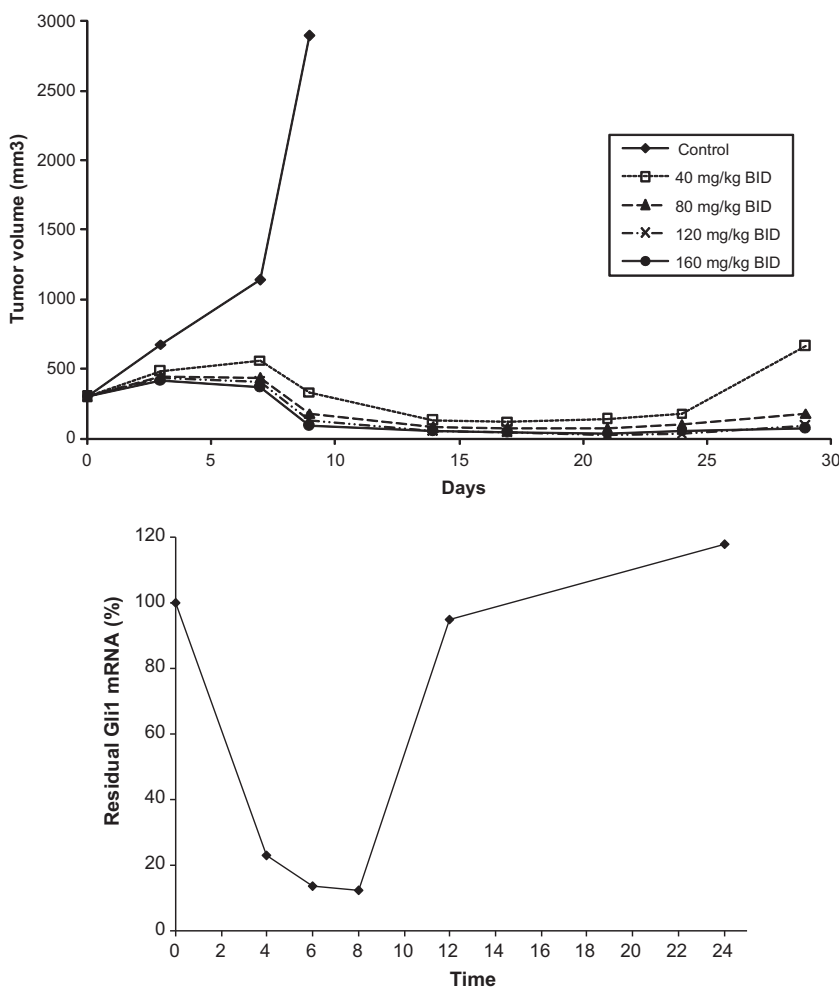


Figure 4. Efficacy of **47** in medulloblastoma bearing mice,¹³ following oral dosing at 40, 80, and 160 mg/kg bid as suspension in 0.24% SDS/0.5% Methocel. PD of **47** in tumor biopsies from medulloblastoma bearing mice following a single oral 80 mg/kg dose.

10% body weight loss, and no visible physical signs or mortality. Tumor growth inhibition was observed in all groups (Fig. 2), with regression being observed at doses of 80 mg/kg bid and upwards. It appears that in this preclinical model it is necessary to inhibit the pathway completely for 24 h in order to see optimal anti-tumor activity, as 80 mg/kg qd gives only modest tumor growth inhibition, and this is inferior to the same quantity of compound administered twice-a-day (i.e., 40 mg/kg bid). Similar findings have been seen by other groups.¹⁴ Parallel, pharmacodynamic (PD) studies in tumor bearing mice demonstrated that following a single oral 80 mg/kg dose strong inhibition of the Hh-pathway is observed in tumor biopsies, causing a >80% reduction of Gli-1 mRNA between 4 and 12 h.

Despite the encouraging profile, and the demonstration of in vivo anti-tumor activity concern about possible epimerization of the hydantoin ring stimulated deeper investigation.¹⁵ Indeed epimerization occurs in both rat and human plasma (Fig. 3), with around 30% conversion within 3 h to a biologically active epimer (Smo binding $IC_{50} = 50$ nM (2% FCS)).

In order to avoid this epimerization, attempts were made to block this position by the addition of a methyl group (Scheme 2). The hydantoin scaffold **47** could readily be alkylated in excellent yield by adding LiHMDS to a thoroughly degassed solution of **27** in THF at -78 °C, and quenching with MeI. The diastereomers were separated by chiral SFC chromatography on a Chiralpak AD-H column eluting with 15% IPA/ CO_2 to give first 8S-diastereomer **28** and then 8R-diastereomer **29**. Boc-deprotection and urea formation readily gave **46** and **45**, the direct analogues of **4** and **9**. Interestingly, unlike the unsubstituted compounds where there was only a two-fold difference in activity between diastereomers, in the case of the methylated scaffold there was a striking difference. Whilst **46** displayed comparable activity to **4** in the Smo binding assays, $IC_{50} = 19$ and 21 nM respectively in 2% FCS, and $IC_{50} = 60$ and 70 nM in 20% NHS, the other diastereomer **45** proved to be more than 50-fold less active ($IC_{50} = 1.1$ μ M). Encouraged by this result, **47** the direct analogue of **42** was prepared from key intermediate **31** using the phenyl carbamate **33** generated in situ. This derivative maintained all the beneficial characteristics of the unsubstituted compound (activity, selectivity, PK and activity in vivo), whilst eliminating the potential for epimerization. In fact, **47** proved to be an extremely potent Smo antagonist displaying $IC_{50} = 17$ nM in the Light2 cells, whilst binding to Smo with $IC_{50} = 22$ nM in 20% NHS. Indeed, **47** inhibited the medulloblastoma proliferation with $CC_{50} = 0.4$ nM.¹⁶

No unwanted off-target activities were detected at 10 μ M on a panel of over 150 enzyme and receptor binding assays, while profiling on the cardiac ion channels showed only minimal functional inhibition of hERG (27% inh. at 30 μ M), and I_{Na} (45% block at 30 μ M). In an anesthetized, vagotomized CV dog study no significant changes to CV or hemodynamic parameters were measured following iv infusion ($C_{max} = 16.0$ μ M). Furthermore, no inhibition of CYP450s 2D6, 2C9 or 3A4 was observed ($IC_{50} > 40$ μ M).

The pharmacokinetic properties of **47** were similar to those of the unsubstituted derivative. In rats, **47** displayed good PK properties, with low clearance ($Cl = 22$ mL/min/kg), $T_{1/2} = 5.1$ h, and good oral bioavailability ($F = 40\%$). The dog PK of **47** is acceptable, and despite the high Cl_{int} in microsomes, in vivo the compound displays $Cl = 21$ mL/min/kg and good oral bioavailability ($F = 46\%$).

Efficacy in the primary mouse medulloblastoma allograft model was also demonstrated at well tolerated doses (Fig. 4). Daily oral

doses of **47** at 40, 80, and 160 mg/kg bid all gave rise to sustained tumor regression and no body weight loss or adverse effects were observed in any group. Efficacious exposures correspond to $AUC_{0-inf} = 10.9$, 24.6, and 133 μ M h with $C_{max} = 7.8$, 19.6 and 41.7 μ M. Pharmacodynamic studies in tumor biopsies revealed **47** leads to a time-dependent down-regulation of Gli-1 mRNA with 77% down regulation at 4 h, and >85% pathway inhibition at 6 and 8 h following dosing at 80 mg/kg.

In summary, a novel series of potent bicyclic hydantoin Smo antagonists has been developed, with clean off-target profiles and good pharmacokinetic properties in preclinical species. This series of compounds demonstrates target engagement in tumor biopsies, and anti-tumor activity in mouse allograft models dependent on the Hh signalling pathway. On the basis of this data MK-5710 (**47**) was selected for further development.

References and notes

- Rubin, L. L.; de Sauvage, F. J. *Nat. Rev. Drug Disc.* **2006**, *5*, 1026.
- Xie, J. *Curr. Oncol. Rep.* **2008**, *10*, 107.
- Gallinari, P.; Filocomo, G.; Jones, P.; Pazzaglia, S.; Steinkühler, C. *Exp. Opin. Drug Discov.* **2009**, *4*, 525.
- Ingham, P. W.; McMahon, A. P. *Genes Dev.* **2001**, *15*, 3059.
- Peukert, S.; Miller-Moslin, K. *ChemMedChem* **2010**, *5*, 500.
- Robarge, K. D.; Brunton, S. A.; Castaneda, G. M.; Cui, Y.; Dina, M. S.; Goldsmith, R.; Gould, S. E.; Guichert, O.; Gunzner, J. L.; Halladay, J.; Jia, W.; Khojasteh, C.; Koehler, M. F. T.; Kotkow, K.; La, H.; LaLonde, R. L.; Lau, K.; Lee, L.; Marshall, D.; Marsters, J. C.; Murray, L. J.; Qian, C.; Rubin, L. L.; Salphati, L.; Stanley, M. S.; Stibbard, J. H. A.; Sutherlin, D. P.; Ubhayaker, S.; Wang, S.; Wong, S.; Xie, M. *Bioorg. Med. Chem. Lett.* **2009**, *19*, 5576.
- Von Hoff, D. D.; LoRusso, P. M.; Rudin, C. M.; Reddy, J. C.; Yauch, R. L.; Tibes, R.; Weiss, G. J.; Borad, M. J.; Hann, C. L.; Brahmer, J. R.; Mackey, H. M.; Lum, B. L.; Darbonne, W. C.; Marsters, J. C.; de Sauvage, F. J., Jr.; Low, J. A. N. *Engl. J. Med.* **2009**, *361*, 1164.
- Malancona, S.; Altamura, S.; Filocomo, G.; Kinzel, O.; Martin Hernandez, J. I.; Rowley, M.; Scarpelli, R.; Steinkühler, C.; Jones, P. *Bioorg. Med. Chem. Lett.* **2011**, *21*. doi:10.1016/j.bmcl.2011.06.024.
- Compound 1 was separated following two sequential runs, on Chiralpak IB column using 30% MeOH (0.2% DEA) as modified, and subsequently on Chiralcel OJ column using 60% MeOH (0.2% DEA).
- Taipale, J.; Chen, J. K.; Cooper, M. K.; Wang, B.; Mann, R. K.; Milenkovic, L.; Scotts, M. P.; Beachy, P. A. *Nature* **2000**, *406*, 1005; Frank-Kamenetsky, M.; Zhang, X. M.; Bottega, S.; Guicherit, O.; Wichterle, H.; Dudek, H.; Bumcrot, D.; Wang, F. Y.; Jones, S.; Shulok, J.; Rubin, L. L.; Porter, J. A. *J. Biol.* **2002**, *1*, 10.
- Chen, J. K.; Taipale, J.; Cooper, M. K.; Beachy, P. A. *Genes Dev.* **2002**, *16*, 2743.
- Newman, P. In *Optical Resolution Procedures for Chemical Compounds. Vol. 1. Amines and Related Compounds*; Optical Resolution and Information Center: Manhattan College, Riverdale, NY, 1978; p. 120.
- Pazzaglia, S.; Tanori, M.; Mancuso, M.; Rebessi, S.; Leonardi, S.; Di Majò, V.; Covelli, V.; Atkinson, M. J.; Hahn, H.; Saran, A. *Oncogene* **2006**, *25*, 1165; Pazzaglia, S.; Tanori, M.; Mancuso, M.; Gessi, M.; Pasquali, E.; Oliva, M. A.; Rebessi, S.; Di Majò, V.; Covelli, V.; Giangaspero, F.; Saran, A. *Oncogene* **2006**, *25*, 5575.
- Miller-Moslin, K.; Peukert, S.; Jain, R. K.; McEwan, M. A.; Karki, R.; Llamas, L.; Yusuff, N.; He, F.; Li, Y.; Sun, Y.; Dai, M.; Perez, L.; Michael, W.; Sheng, T.; Lei, H.; Zhang, R.; Williams, J.; Bourret, A.; Ramamurthy, A.; Yuan, J.; Guo, R.; Matsumoto, M.; Vattay, A.; Maniara, W.; Amaral, A.; Dorsch, M.; Kelleher, J. F. *J. Med. Chem.* **2009**, *52*, 3954.
- (a) Reist, M.; Carrupt, P.-A.; Testa, B.; Lehmann, S.; Hansen, J. J. *Helv. Chim. Acta* **1996**, *79*, 767; (b) Moghaddam, M. F.; Bogdanffy, M. S.; Brown, A.; Ford, K.; Shalaby, L. *Drug Metab. Dispos.* **2002**, *30*, 47; (c) Moghaddam, M. F.; Brown, A.; Budevskaa, B. O.; Lam, Z.; Payne, W. G. *Drug Metab. Dispos.* **2001**, *29*, 1162; (d) Veniant, M. M.; Hale, C.; Hungate, R. W.; Gahm, K.; Emery, M. G.; Jona, J.; Joseph, S.; Adams, J.; Hague, A.; Moniz, G.; Zhang, J.; Bartberger, M. D.; Li, V.; Syed, R.; Jordan, S.; Komorowski, R.; Chen, M. M.; Cupples, R.; Kim, K. W.; Jean, D. J.; Johansson, L.; Henriksson, M. A.; Williams, M.; Vallgarda, J.; Fotsch, C.; Wang, M. J. *J. Med. Chem.* **2010**, *53*, 4481.
- The stereochemistry of the 8 α -methyltetrahydroimidazo[1,5-a]pyrazine-1,3(2H,5H)-dione scaffold was confirmed by independent synthesis starting from α -aminomethylalanine methyl ester. Yi, H.; Hegedus, L. S. *J. Org. Chem.* **1997**, *62*, 3586.